

Supporting Information

# Design of 3D Carbon Nanotube Monoliths for Potential-Controlled Adsorption

Dennis Röcker <sup>\*,†</sup>, Tatjana Trunzer <sup>†</sup>, Jasmin Heilingbrunner, Janine Rassloff, Paula Fraga-García and Sonja Berensmeier <sup>\*</sup>

Technical University of Munich, Department of Mechanical Engineering, Bioseparation Engineering Group, Boltzmannstraße 15, 85748 Garching

<sup>\*</sup> Correspondence: d.roecker@tum.de (D.R.); s.berensmeier@tum.de (S.B.)

<sup>†</sup> These authors contributed equally to this work.

*Materials and Methods*

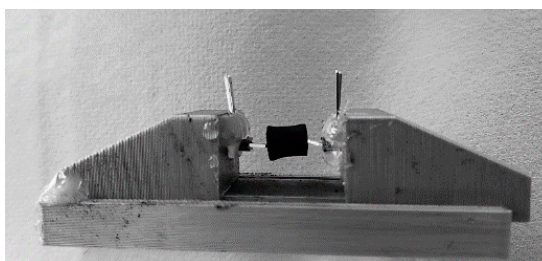
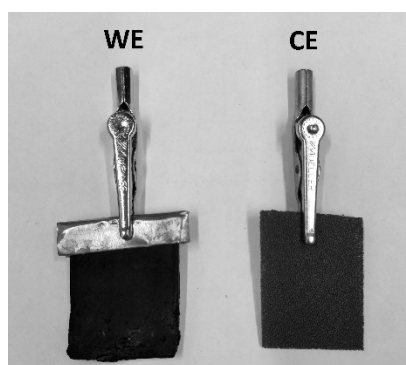
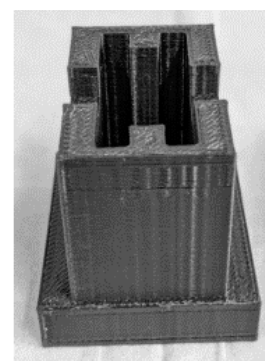


**Figure S1.** Test rig for conductivity measurements on cylindrical monoliths (density:  $\sim 0.3 \text{ g cm}^{-3}$ ; length:  $\sim 12 \text{ mm}$ ;  $\varnothing \sim 7 \text{ mm}$ ).



(a)



(b)

**Figure S2.** Electrode contacting (a) Left: Planar monolith CNT-K working electrode contacted by a copper sheet. Right: Steel foam counter electrode. Monolith and CE dimensions:  $\sim 35.0 \times 30.5 \times 2.7 \text{ mm}$ . (b) Test rig for potential-controlled adsorption experiments. Within the test rig the electrodes were spaced 5 mm apart. The slots for the containment of the electrodes had the dimensions  $30.5 \times 32.0 \times 5.0 \text{ mm}$ .

## Particle Characterization

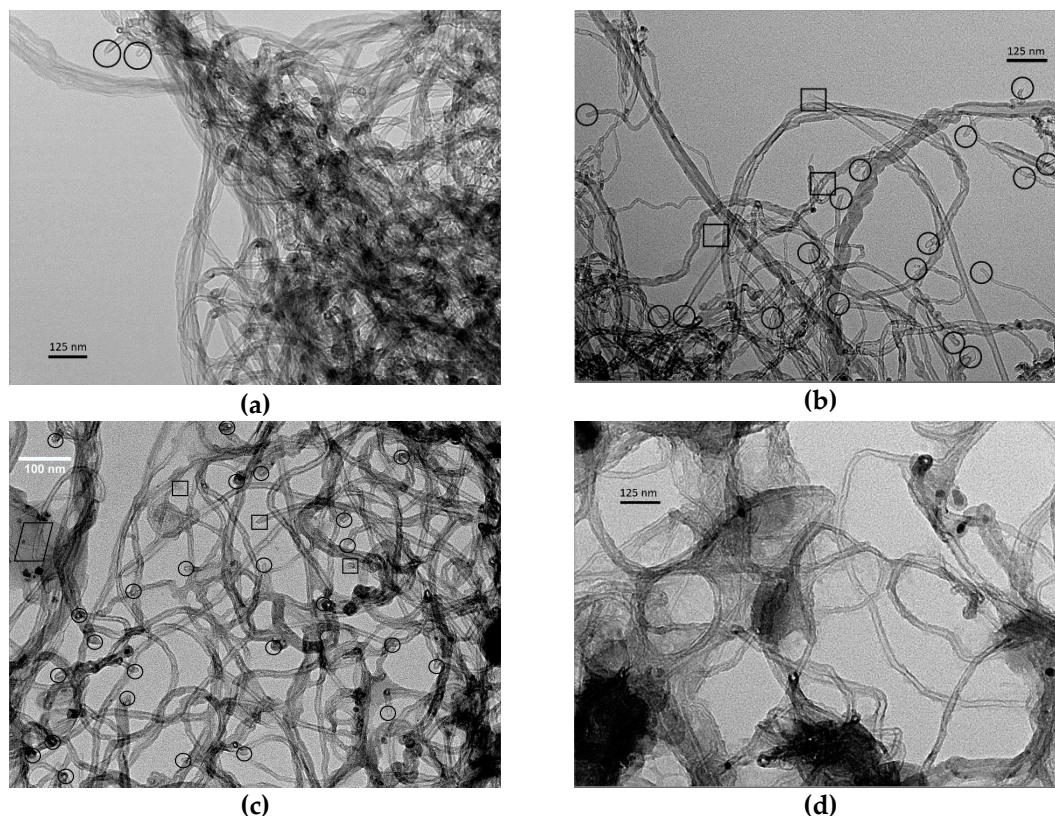


**Figure S3.** Agglomerates of CNT-K after (a) no ultrasonic treatment in DI-water, (b) 6 min ultrasonic treatment in DI-water, (c) oxidation and 6 min ultrasonic treatment, (d) 6 min ultrasonic treatment in SDBS 10 g L<sup>-1</sup>. Closed nanotube ends marked by circles and opened ends marked by squares respectively. Pictures taken by Dr. Sebastian Schwaminger and Chiara Turrina.

CNT-K display a strong agglomeration behavior in DI-water. Most of the CNT-K tubes present closed ends due to the synthesis process (see Figure S3) [1, 2]. Upon ultrasonication, the nanotubes can be spatially separated as displayed in Figure 34b. No considerable increase in opened and fractured nanotubes upon oxidation and ultrasonication could be observed through TEM imaging. Ultrasonication in SDBS (see Figure S3d) lead towards strong separation of the tubes. The blurred outline of the tubes can be attributed towards the accumulation of SDBS as it strongly adsorbs on the nanotubes surface [3, 4].

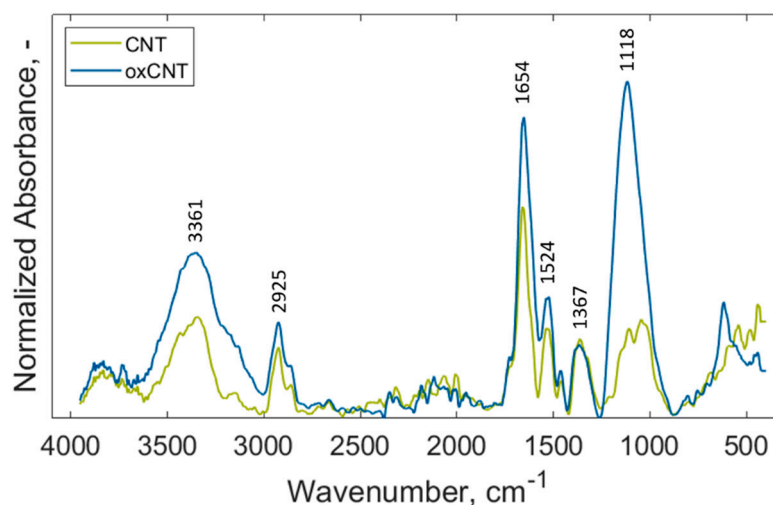


**Figure S4.** FTIR spectra of untreated (green) and oxidized (blue) CNT particles.

The peaks visible for purified CNTs indicate the presence of already oxidized species, possibly originated by the synthesis or purification of the nanotubes [5]. Nonetheless, as the peak intensity is considerably weaker compared to the oxidized species, an apparent effect of the surface oxidation is noticeable. A first broad peak present at 3361  $\text{cm}^{-1}$  corresponds to strong  $\text{-OH}$  stretching vibrations originated by  $\text{-OH}$  substituents of carboxyl groups, isolated alcohol groups, or water. The peak at 2925  $\text{cm}^{-1}$  originates from the stretching of  $\text{C-H}$  bonds in carbonaceous material. A series of peaks ranging from 1700  $\text{cm}^{-1}$  – 1500  $\text{cm}^{-1}$  indicates the presence of  $\text{C=O}$  groups in different configurations, while the peak visible at 1367 corresponds to  $\text{C=C}$  vibrations of the CNT backbone [6]. The pronounced peak at 1118  $\text{cm}^{-1}$  can be associated with  $\text{C-O}$  stretching and indicates the presence of ester, ether, and alcohol groups on the surface [6]. Upon treatment in concentrated  $\text{HNO}_3$  a more dominant rise of the  $\text{C=O}$  stretch was reported by Stobinski *et al.* [7]. Nonetheless, for CNT-K, a considerable increase in the  $\text{C-O}$  stretch can be observed upon oxidation, showing the augmented presence of oxidized surface groups. Similar results were obtained by Avilés *et al.*, for the oxidation of MWCNTs in 3 M  $\text{HNO}_3$  [5].

#### Monolith Characterization

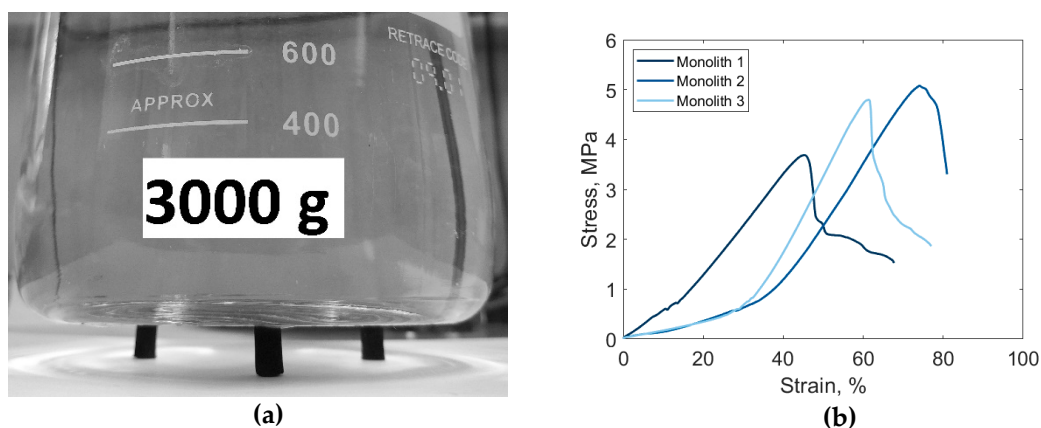


**Figure S5.** Mechanical strength of cylindrical and planar monoliths. (a) Three cylindrical monoliths (density 0.3  $\text{g cm}^{-3}$ , weight  $\sim 0.19$  g per monolith) supporting a total weight of 3000 g and (b) tensile strength of planar monoliths.

The synthesized monoliths are characterized by a high structural strength. For instance, 3 cylindrical monoliths with a density of 0.3  $\text{g cm}^{-3}$  can support a counterweight of

3000 g without signs of structural collapse, showing superior stability to other carbon aerogels tested under similar conditions [8–10]. Planar monoliths displayed a maximum strength of 4 to 5 N mm<sup>-1</sup> proving, that the synthesis of monoliths in different shapes is possible by a mold-pressing and heat drying approach.

## References

1. Trunzer T, Stummvoll T, Porzenheim M et al. (2020) A Carbon Nanotube Packed Bed Electrode for Small Molecule Electrosorption: An Electrochemical and Chromatographic Approach for Process Description. *Applied Sciences* 10:1133. <https://doi.org/10.3390/app10031133>
2. Frackowiak E, Metenier K, Bertagna V et al. (2000) Supercapacitor Electrodes from Multiwalled Carbon Nanotubes. *Appl Phys Lett* 77:2421–2423. <https://doi.org/10.1063/1.1290146>
3. Niyogi S, Boukhalifa S, Chikkannanavar SB et al. (2007) Selective Aggregation of Single-walled Carbon Nanotubes via Salt Addition. *J Am Chem Soc* 129:1898–1899. <https://doi.org/10.1021/ja068321j>
4. Clark MD, Subramanian S, Krishnamoorti R (2011) Understanding Surfactant Aided Aqueous Dispersion of Multi-walled Carbon Nanotubes. *J Colloid Interface Sci* 354:144–151. <https://doi.org/10.1016/j.jcis.2010.10.027>
5. Avilés F, Cauich-Rodríguez JV, Moo-Tah L et al. (2009) Evaluation of Mild Acid Oxidation Treatments for MWCNT Functionalization. *Carbon* 47:2970–2975. <https://doi.org/10.1016/j.carbon.2009.06.044>
6. Tucureanu V, Matei A, Avram AM (2016) FTIR Spectroscopy for Carbon Family Study. *Crit Rev Anal Chem* 46:502–520. <https://doi.org/10.1080/10408347.2016.1157013>
7. Stobinski L, Lesiak B, Kövér L et al. (2010) Multiwall Carbon Nanotubes Purification and Oxidation by Nitric Acid Studied by the FTIR and Electron Spectroscopy Methods. *Journal of Alloys and Compounds* 501:77–84. <https://doi.org/10.1016/j.jallcom.2010.04.032>
8. Kohlmeyer RR, Lor M, Deng J et al. (2011) Preparation of Stable Carbon Nanotube Aerogels with High Electrical Conductivity and Porosity. *Carbon* 49:2352–2361. <https://doi.org/10.1016/j.carbon.2011.02.001>
9. Bryning MB, Milkie DE, Islam MF et al. (2007) Carbon Nanotube Aerogels. *Adv Mater* 19:661–664. <https://doi.org/10.1002/adma.200601748>
10. Shen Y, Du A, Wu X-L et al. (2016) Low-cost Carbon Nanotube Aerogels with Varying and Controllable Density. *J Sol-Gel Sci Technol* 79:76–82. <https://doi.org/10.1007/s10971-016-4002-7>